Published in final edited form as:
Curr Urol Rep. 2010 May ; 11(3): 180–190. doi:10.1007/s11934-010-0105-9.

Imaging Prostate Cancer: An Update on Positron Emission Tomography and Magnetic Resonance Imaging

Kirsten Bouchelouche,
PET & Cyclotron Unit, PET 3982, Rigshospitalet, University of Copenhagen, Blegdamsvej 9, 2100 Copenhagen, Denmark

Baris Turkbey,
Molecular Imaging Program, Center for Cancer Research, National Cancer Institute, National Institutes of Health, Bethesda, MD, USA

Peter Choyke, and
Molecular Imaging Program, Center for Cancer Research, National Cancer Institute, National Institutes of Health, Bethesda, MD, USA

Jacek Capala
Molecular Targeting Section, Radiation Oncology Branch, Center for Cancer Research, National Cancer Institute, National Institutes of Health, Bethesda, MD, USA

Kirsten Bouchelouche: bouchelouche@mail.tele.dk

Abstract

Prostate cancer is a common cancer in men and continues to be a major health problem. Imaging plays an essential role in the clinical management of patients. An important goal for prostate cancer imaging is more accurate disease characterization through the synthesis of anatomic, functional, and molecular imaging information. Developments in imaging technologies, specifically magnetic resonance imaging (MRI) and positron emission tomography (PET)/computed tomography (CT), have improved the detection rate of prostate cancer. MRI has improved lesion detection and local staging. Furthermore, MRI allows functional assessment with techniques such as diffusion-weighted MRI, MR spectroscopy, and dynamic contrast-enhanced MRI. The most common PET radiotracer, ^{18}F-fluorodeoxyglucose, is not very useful in prostate cancer. However, in recent years other PET tracers have improved the accuracy of PET/CT imaging of prostate cancer. Among these, choline (labeled with ^{18}F or ^{11}C), ^{11}C-acetate, and ^{18}F-fluoride have demonstrated promising results, and other new radiopharmaceuticals are currently under evaluation in preclinical and clinical studies.

Keywords

Prostate cancer; Imaging; Positron emission tomograph; PET; PET/CT; Magnetic resonance imaging; MRI; Magnetic resonance spectroscopy; MRS; Dynamic contrast-enhanced MRI; Diffusion-weighted MRI

Correspondence to: Kirsten Bouchelouche, bouchelouche@mail.tele.dk.

Disclosure No potential conflicts of interest relevant to this article were reported.

Introduction

In developed countries, prostate cancer is the second most frequently diagnosed cancer, and the third most common cause of death from cancer in men [1••]. Clinically, prostate cancer is diagnosed as local or advanced. At present, diagnosis is based on examination of histopathological or cytological specimens from the gland. The most common way to obtain the necessary tissue specimen is by several systematic transrectal core biopsies, with guidance by transrectal ultrasound (TRUS). Prostate cancer usually responds to androgen deprivation therapy, but on average, after 12 to 18 months, malignant cells become resistant [2]. Many novel therapeutic approaches are in development, including new cytotoxic agents, antiproliferative therapies, immune-based agents, and antiangiogenic agents [1••, 2]. Other new treatment modalities in advanced prostate cancer may involve targeted radionuclide therapy (TRT) [3•, 4•].

Currently, prostate cancer is classified into three risk groups (low, intermediate, or high) based on serum prostate-specific antigen (PSA) level, Gleason score, and clinical stage. These groups are used as a guide to make treatment decisions. TNM classification is the reference standard for staging prostate cancer. Imaging plays an important role in staging, which is crucial for choosing the optimal treatment strategy in prostate cancer [5••, 6•]. Furthermore, imaging is a powerful modality in staging because most imaging techniques are noninvasive or minimally invasive, can provide real-time data, and allow repeated measurements. The goals of imaging modalities depend on the clinical state of prostate cancer [7•]. For initial prostate evaluation (no cancer diagnosis), imaging may distinguish cancer from benign tissue. In patients with newly diagnosed prostate cancer, imaging should be used to identify extent of both localized and metastatic disease, prognosticate, and evaluate effects of treatment. In patients with biochemical recurrence (rising PSA), imaging should identify extent of both localized and metastatic disease to guide therapy. In patients with clinical metastases, imaging should determine extent of metastatic disease, assess treatment response, identify patients with a particular biologic profile, prognosticate, and determine pharmacodynamics of targeted therapy. Other important imaging goals include shorter duration of phase 2 trials to evaluate new drugs and accelerated approval in phase 3 trials.

Conventional imaging, including computed tomography (CT), magnetic resonance imaging (MRI), and ultrasound, is currently used to detect organ-confined or metastatic disease for staging and determining prognosis in prostate cancer patients. However, there is need for improvement in the use of imaging for determining tumor grade, staging, identifying minimal metastatic disease, and distinguishing lethal from nonlethal disease. This review summarizes recent developments in positron emission tomography (PET)/CT and MRI of prostate cancer.

PET

PET is a tomographic technique that computes the three-dimensional (3D) distribution of radioactivity based on the detection of photons resulting from annihilation of positrons that are emitted by positron emitter-labeled radiotracers. PET allows noninvasive quantitative assessment of biochemical and functional processes. In contrast to PET, CT uses an eternal X-ray beam to generate tomographic images. CT allows the visualization of morphological and anatomic structures with a high anatomical resolution. Anatomical and morphological information derived from CT can be used to increase the precision of localization, assessment of extent, and characterization of lesions detected by PET. Integrated PET/CT combines PET and CT in a single imaging device and allows morphological and functional imaging to be carried out in a single imaging procedure.

The most commonly used PET radiotracer at present is the glucose analogue ^{18}F-fluorodeoxyglucose (FDG), a marker of glucose metabolism. To date, most oncologic clinical studies have used ^{18}F-FDG for PET/CT, and ^{18}F-FDG PET/CT is now an established imaging modality that has been extensively validated in routine clinical practice of several cancers. However, not all cancers are ^{18}F-FDG avid, including most prostate cancers; in the recent years, new and more promising PET tracers are being evaluated in prostate cancer.

PET Tracers and Prostate Cancer

FDG

FDG accumulation in tissue is proportional to the amount of glucose utilization. Increased consumption of glucose is a characteristic of most cancers and is in part related to overexpression of the GLUT-1 glucose transporters and increased hexokinase activity. Once inside the cell, FDG is phosphorylated by hexokinase into FDG-6-phosphate, which is not metabolized and accumulates intracellularly. Unfortunately, a large fraction of prostate cancer has a relatively slow metabolic rate and expresses fewer GLUT-1 binding sites, leading to lower ^{18}F-FDG uptake compared with other cancers. Thus, the results of ^{18}F-FDG PET/CT in detecting prostate cancer have been mixed [8•, 9]. To improve the usefulness of PET/CT in prostate cancer detection, molecular PET probes with higher sensitivity and specificity are being developed and validated. Specifically, PET tracers such as ^{11}C-acetate, ^{11}C-choline, and ^{18}F-choline have been investigated as alternatives to ^{18}F-FDG. In addition, other biomarkers are being developed and tested in preclinical and clinical studies [3•, 6•].

Choline

Choline is incorporated into tumor cells by conversion into phosphorylcholine, which is trapped inside the cell. This is followed by synthesis of phosphatidylcholine, which constitutes a main component of cell membranes. Because most tumor cells proliferate very quickly, the biosynthesis of cell membranes also is very rapid, resulting in increased uptake of choline and upregulation of the enzyme choline kinase. Thus, the uptake of choline in tumors corresponds to the rate of tumor cell proliferation. Choline has been labeled with ^{18}F and ^{11}C for PET/CT imaging in prostate cancer (Fig. 1). Because ^{11}C has a very short half-life of 20 min, an onsite cyclotron and a radiochemistry laboratory with experienced staff is necessary for using this radionuclide for PET/CT imaging in patients. Several PET/CT studies have demonstrated choline useful for detection of prostate cancer [3•, 5••, 6•, 7•].

Acetate

Acetate uptake in tumor cells is proportional to lipid synthesis. Acetate is metabolized and incorporated into the cellular lipid pool, mostly phosphatidylcholine (incorporated in the cell membrane) and neutral lipids. An increase in fatty acid synthesis and an overexpression of the key enzyme fatty acid synthase have been demonstrated in prostate cancer [10]. Acetate labeled with ^{11}C is used for PET/CT imaging of prostate cancer (Fig. 2) [3•, 5••, 6•, 7•].

Amino Acids

For imaging of amino acid transport, ^{11}C-methionine has been used in prostate cancer [11]. Uptake of ^{11}C-methionine is proportional to the amino acid transport and, to some extent, protein synthesis. In cancer, methionine uptake has been correlated with the amount of viable tumor tissue. Anti-1-amino-3-^{18}F-fluorocyclobutane-1-carboxylic acid (^{18}F-FACBC) is a synthetic l-leucine analog that is taken up by amino acid transporters into cancer cells. In a pilot study, limited bladder excretion was demonstrated, and ^{18}F-FACBC PET/CT was able to detect both localized disease and recurrence of prostate cancer [12].

Androgen Receptor

With respect to androgen receptor imaging, PET tracers such as 16β-^{18}F-fluroro-5α-dihydrotestosterone (^{18}F-FDHT) targeted to the androgen receptor have been developed and evaluated [13]. The androgen receptor plays an important role in the growth and proliferation of prostate cancer as well as modulation of androgen status. Antiandrogen is widely used in treatment of prostate cancer. ^{18}F-FDHT PET/CT may be useful in monitoring treatment response; however, this has to be investigated further.

PSMA

In prostate cancer there is increasing evidence that prostate-specific membrane antigen (PSMA) may be a target for both imaging and therapy [14••, 15••]. PSMA is highly expressed by virtually all prostate cancers, and the expression increases with tumor aggressiveness, androgen independence, metastatic disease, and disease recurrence. The first clinical agent targeting PSMA in prostate cancer was performed with ProstaScint (capromab pendetide; EUSA Pharma, Oxford, England) [14••]. The relatively poor results of the initial studies using ProstaScint may be due to the fact that capromab pendetide recognizes an internal epitope of PSMA, and hence detects only necrotic tissue [7•]. More recently, radiolabeled monoclonal antibodies (mAbs) that bind to the *extracellular* domain of PSMA have been developed. Among these, the humanized version of J591 has had promising results in imaging and TRT of prostate cancer [15••, 16, 17]. In the past few years, other mAbs that target PSMA for molecular imaging have been developed and tested in in vivo studies [18, 19•, 20••]. Low-molecular-weight, radiopharmaceutical-based imaging agents may provide superior pharmacokinetics for imaging than radiolabeled antibodies, and this small molecule approach has demonstrated promising results for PET/CT and single photon emission computed tomography (SPECT)/CT imaging [15•, 21••]. Furthermore, PSMA is an attractive target for TRT in advanced prostate cancer.

HER2

Overexpression of the HER2 protein and amplification of the *HER2* gene have been implicated in tumor development and progression, and is associated with a poor prognosis in several types of cancer. There is increasing evidence that HER2 also plays a role in advanced prostate cancer [3•, 4•]. Monoclonal antibodies such as trastuzumab and pertuzumab, or the small scaffold Affibody molecule are used as HER2-targeting agents. For imaging purposes, these agents are labeled with positron- or gamma-emitting radionuclides for PET or SPECT imaging, respectively. Recently, a HER2-binding Affibody molecule has been labeled with ^{18}F for in vivo monitoring of the HER2 expression by PET, and the same tracer has been used to assess the changes of HER2 expression following therapeutic intervention [22••]. Increased HER2 expression in prostate cancer represents a target for imaging with PET/CT and SPECT/CT, as well as for TRT in metastatic disease.

Fluoride

Bone is the most common site for prostate cancer metastases. Bone scintigraphy uses ^{99m}Tc-labeled methylene diphosphonate that is incorporated into hydroxyapatite, the principal component of bone cortex. However, this is not a specific agent for detection of malignancy. For imaging of osteoblastic activity, ^{18}F-fluoride may be used in PET/CT studies. ^{18}F-fluoride is highly effective in detection of bone metastases, and uptake in malignant bone lesions reflects the increase in regional blood flow and bone turnover [10].

PET/CT Imaging in Prostate Cancer

Diagnosis and Detection

For primary diagnosis of prostate cancer, a pathologic examination of multiple core biopsies is used. TRUS is primarily used for guiding the biopsy needle to the desired anatomical locations in order to estimate prostatic volume and assist systematically biopsy sampling. ^{18}F-FDG has low sensitivity for detection of cancer in the prostate gland and is not very useful for diagnosis, assessment of local organ-confined cancer, or extracapsular extension. Furthermore, similarities in the ^{18}F-FDG uptake in prostate tumors and benign prostatic hyperplasia (BPH) have been demonstrated [8•]. Additionally, intense tracer activity in the bladder may mask uptake in the prostate and interferes with the identification of pelvic lymph node metastases. New radiotracers that target tumor proliferation, membrane turnover, and amino acid transport are currently under investigation. Choline, labeled with ^{18}F or ^{11}C, and ^{11}C-acetate are examples of such tracers that are being investigated. ^{11}C-acetate is metabolized in various organs and has little urinary excretion, allowing PET imaging of the pelvis without interference with tracer activity in the bladder. Although ^{11}C-acetate PET/CT has been demonstrated to be useful in the diagnosis, staging, and restaging of prostate cancer, prospective clinical trials are needed to properly evaluate its role in localized disease [8•]. Similar to ^{11}C-acetate, ^{11}C-choline has limited urinary excretion, and is thus more suitable for PET imaging of the prostate than ^{18}F-FDG. Several studies have demonstrated ^{11}C-choline to be useful for PET/CT imaging of prostate cancer [23, 24]. However, false-positive findings may occur due to an overlap of ^{11}C-choline uptake between benign and malignant processes in the prostate gland [24]. The very short half-life of ^{11}C (20 min) may make it less practical than ^{18}F (110 min) for using it as a choline radiolabel because of logistic issues. On the other hand, ^{18}F-choline is excreted in the urine and may, therefore, be less suitable for detection of malignancy in the prostate gland.

Staging

^{18}F-FDG PET/CT demonstrates limited detection rate of malignant lymph node involvement in the pelvis, but it may be used in some advanced metastatic cases with poor response to therapy, or rising PSA during therapy. Several PET/CT studies using choline and acetate have demonstrated promising results in detecting metastatic prostatic disease [3•, 8•]. It has been shown that the detection rate of malignancy depends on PSA level [25, 26••]. The results obtained with choline and acetate, although much better than FDG, have to be evaluated further in larger prospective trials to properly establish their role in prostate cancer. Currently, at least two large prospective trials are investigating the feasibility of ^{18}F-choline PET/CT for preoperative N-staging of prostate cancer. The utility of other tracers, ie, ^{18}F-FACBC, radiolabeled agents targeting PSMA, ^{18}F-FLT (a marker of cell proliferation), and ^{18}F-DHT, remains to be evaluated further.

Recurrence

After definitive radical prostatectomy or radiation therapy, biochemical recurrence (rising PSA) is often the first sign of prostate cancer recurrence. Rising PSA most often precedes clinical sign of recurrence by years. The time to recurrence after radical prostatectomy depends on preoperative pathologic stage, Gleason score, and postoperative PSA doubling time. It is important to determine whether the recurrence is local and/or is in distant organs in order to select the appropriate therapy. Due to the typically slow growth rate of prostate tumors, ^{18}F-FDG is not the optimal tracer for detection of recurrence. In some cases of recurrence, ^{18}F-FDG PET/CT may demonstrate both local and distant recurrence. However, the newer tracers, ^{18}F-choline, ^{11}C-choline, and ^{11}C-acetate, demonstrate much higher

detection rate of local recurrence, regional lymph node involvement, and/or distant organ involvement after radical prostatectomy and radiation therapy [3•, 7•, 26••, 27].

Bone Metastases

Currently, ^{99m}Tc-MDP bone scan is the standard method for detection of bone metastases in prostate cancer patients. SPECT/CT may improve the detection of bone metastases compared with conventional planar bone scintigraphy because of the higher sensitivity of modern SPECT/CT cameras and the better resolution of SPECT/CT compared with projection scintigraphy. It has been demonstrated that ^{18}F-fluoride PET/CT is superior to ^{99m}Tc planar imaging and SPECT/CT for detection of bone metastases [28]. In a recent prospective study, the potential value of ^{18}F-choline was compared with ^{18}F-fluoride PET/CT for the detection of bony metastases from prostate cancer [29••]. The sensitivity, specificity, and accuracy of PET/CT in the detection of bone metastases were 81%, 93%, and 86% for ^{18}F-fluoride, and 74%, 99%, and 85% for ^{18}F-choline, respectively.

MRI

An accurate and noninvasive imaging method of determining the location, extent, and biological potential of prostate cancer could improve patient outcome and prognosis by directing therapy more accurately. Current therapies such as radical prostatectomy and radiotherapy usually treat the whole gland; however, by depicting the exact location of the cancer and its margins, therapies may ultimately be targeted to the cancer by imaging, thus sparing the patient unwanted treatment side effects such as incontinence or impotence. With the advent of PSA screening, prostate cancer is increasingly detected while still confined to the prostate gland. Effective therapy depends on accurate localization and staging of prostate cancer. In the case of surgery, accurate localization and staging permit sparing of unaffected neurovascular bundles with preservation of erectile function. In the case of radiation therapy, accurate localization and staging permit adjustment of dose to boost the tumor and minimize exposure to periprostatic tissues, thus reducing side effects. Accurate localization of prostate cancer paves the way for innovative, minimally invasive therapies and it may be possible to reduce the number of men undergoing biopsy or to improve the diagnostic yield of prostate biopsies by including an imaging method in the diagnostic workup [30]. Despite considerable advances in technology, prostate cancer cannot be reliably detected by current conventional imaging modalities such as TRUS and CT [31, 32]. However, MRI at high field strength may provide improved detection of localized disease and more accurate local staging, which may enable focal therapy in the near future.

MRI in Prostate Cancer

MRI provides the best 3D anatomic imaging of the prostate among all the imaging modalities because of its high spatial resolution, multiplanar capabilities, and excellent soft tissue contrast, making it an attractive imaging modality for the prostate gland. The majority of the experience with prostate MRI was obtained at 1.5 Tesla (T) with the combined use of a phased array surface coil and an endorectal coil. Higher field strength magnets (eg, 3 T), with the same combination of coils or with only the phased array surface coil, improve the signal-to-noise ratio (SNR), resulting in higher resolution images with better spatial and spectral differentiation. Conventional prostate MRI depends on two basic sequences, T1- and T2-weighted (T1W, T2W) MRI. On T1W MRI, the prostate gland usually demonstrates diffuse intermediate signal intensity, hence zonal anatomy and tumors cannot be delineated. However, T1W MRI is mainly used to detect the presence of biopsy-related residual hemorrhage, which appears as a hyperintense focus relative to normal prostate peripheral zone. T2W MRI can demonstrate the zonal anatomy clearly. Normally, the peripheral zone (PZ) is high in signal on T2W images, whereas the transition zone (TZ) is generally lower in

signal with considerable heterogeneity. The TZ is separated from the PZ by a "surgical pseudocapsule," which is ill defined, whereas the true surgical capsule appears as a distinct hypointense rim surrounding the PZ. The neurovascular bundles are located at the posterolateral aspect of the true capsule on axial T2W MRI and can demonstrate both high and low signal intensity foci. The seminal vesicles appear as thin-walled hyperintense structures on T2W MRI. On T2W MRI, PZ cancers are usually rounded or ill-defined, low signal intensity foci; however, this pattern can be mimicked by various conditions such as prostatitis, hemorrhage, atrophy, benign hyperplasia, biopsy-related scars, and posttreatment (eg, hormone, ablation) changes (Fig. 3). Cancers of the TZ are often more difficult to detect because the signal characteristics of the normal TZ overlap with those of tumor, and the characteristics of a TZ tumor can be defined as homogenous, low signal intensity lesion with spiculated margins without a capsule, and invasion of the pseudocapsule, with lenticular, urethral, and anterior fibromuscular invasion [33] (Fig. 4). Detection of extracapsular extension (ECE) is quite important for preoperative staging because its presence upstages the patient to T3a and alters the treatment to a more aggressive approach. On T2W MRI, ECE usually appears as a direct extension of the tumor into the hyperintense periprostatic fat tissue, but frank ECE may not be seen in all situations; under those circumstances, the secondary findings should be evaluated, including asymmetry of the neurovascular bundle, envelopment of the neurovascular bundle, contour angulation, irregular gland margin, capsular obscuration or retraction, and obliteration of the rectoprostatic angle. Seminal vesicle invasion can be directly visualized as the extension of tumor from the base of the prostate and the presence of focal low signal intensity within the normally hyperintense seminal vesicles (Fig. 3). T2W MRI alone is reported to have a range of sensitivities of 27% to 100% and specificities of 32% to 99%, whereas the sensitivity and specificity range for local staging and predicting the presence of extracapsular extension is 14.4% to 100% and 67% to 100%, respectively [34–45••]. The wide range of sensitivities and specificities is due to the significant variability of the patient populations, as well as differences in the gold standard (biopsy vs surgery) and the level of diagnostic and technical expertise in different studies.

Diffusion-Weighted MRI

Diffusion-weighted MRI (DW-MRI) is used to generate apparent diffusion coefficient (ADC) maps that rely on the measurement of water diffusion within a tissue. Normal, well-structured glandular prostate tissue tends to allow diffusion of free water molecules due to its acinar glandular configuration, whereas tumors, with their densely packed cells, abundant stroma, and diminished extracellular spaces, tend to have restricted water diffusion, which results in preserved signal within tumors compared with normal tissue on diffusion-weighted images and a drop in signal on ADC maps [46] (Fig. 5). DW-MRI is a time-efficient MR imaging technique and does not require exogenous contrast media. Moreover, it has the capability of revealing prostate cancer not only in the PZ but also in the TZ. DW-MRI demonstrates a wide range of sensitivities and specificities in the literature (57–93.3% and 57–100%, respectively) for tumor detection, depending on the technology used, field strength, imaging parameters, patient selection, and validation method [47–53]. Currently, DW-MRI has a low signal-to-noise ratio (SNR), but the emergence of high field strength magnets, the widespread use of endorectal coils, and parallel imaging approaches will yield better SNR, and therefore, improved spatial/temporal resolution for DW-MRI.

MR Spectroscopy

MR spectroscopy (MRS) is a technique that generates metabolite spectra based on the differing proton resonance frequencies of a limited number of metabolites such as choline, creatine and citrate. Normal prostate tissue is rich in citrate and has relatively low choline and creatine levels while this pattern is reversed in cancers. Owing to the changes in the

metabolite levels within prostate cancer lesions, the ratio of choline to citrate (cho/cit) can be used as an index for detecting malignancy [54, 55] (Fig. 5). During MRS, signal from lipid and water must be suppressed in order to focus on the signals coming from the key metabolites choline, citrate and creatine which resonate respectively at 3.2, 2.6 and 3.0 parts per million with respect to water. Currently, the majority of the experience with prostate MRS is at 1.5 T; however 3 T or higher field magnets may have several advantages. Increased field strength with its higher SNR, enables faster acquisitions, smaller voxels, and more-accurate separation of metabolite peaks (e.g. better separation of creatine and choline peaks).

Dynamic Contrast-Enhanced MRI

Dynamic contrast-enhanced MRI (DCE-MRI) has been used as a biomarker for the diagnosis and follow-up in various tumor types, including prostate cancer. It provides quantitative kinetic parameters reflecting the permeability and flow characteristics of the vessels within a lesion. DCE-MRI is performed with fast MR imaging sequences (mostly gradient-recalled echo) before, during, and after the rapid administration of a low-molecular-weight contrast agent. Enhancement curves generated from DCE-MRI are mathematically fit to a two compartment pharmacokinetic model such as the Toft's model. Tumors show early intense enhancement compared with normal tissue. Moreover, tumors more rapidly de-enhance or washout than do normal tissue. The Toft's model, which attempts to mathematically fit the T1 versus time curve, produces parameters, such as K^{trans} (transendothelial transport of contrast medium from vascular compartment to the tumor interstitium), k_{ep} (reverse transport parameter of contrast medium back to the vascular space), fpV (plasma volume fraction compared with whole tissue volume), and V_e (extravascular, extracellular volume fraction of the tumor [the fraction of tumor volume occupied by EES]), for describing tumor and tissue permeability [56]. Higher-grade tumors tend to have higher K^{trans} and k_{ep} parameters compared with normal surrounding prostate tissue (Fig. 5). Abnormal enhancement patterns are seen in both tumor foci and BPH nodules, making assessment of the central gland difficult [57]. However, it is important to note that smaller and low-grade tumors often do not demonstrate abnormal enhancement on DCE-MRI [58]. For the detection of tumors, DCE-MRI alone has a sensitivity and specificity range of 46% to 96% and 74% to 96%, respectively; however, as always, these ranges are highly dependent on patient selection, technique, and diagnostic criteria [47, 59••, 60–62].

Conclusions

PET/CT in oncology is emerging as an important imaging tool. The most common tracer for PET/CT imaging, ^{18}F-FDG, is not very effective in the detection of localized prostate cancer. These tumors have a relatively slow metabolic rate, and the tracer does not accumulate in the prostate. ^{18}F-FDG PET/CT does, however, become more useful in patients with androgen-independent tumors. PET tracers, such as ^{18}F-choline, ^{11}C-choline, or ^{11}C-acetate, have a much higher detection rate for prostate cancer. The clinical role of choline and acetate in detection of malignancy in the prostate gland, and preoperative N-staging remains to be evaluated further in larger prospective clinical trials. However, both tracers may be useful for detection of distant metastases, and for detection of recurrence, both locally and in distant organs, after initial treatment. ^{18}F-fluoride is a recently rediscovered agent that is useful for detecting bone metastases with greater sensitivity than ^{99m}Tc-MDP and offers the possibility of more reliable quantitation. ^{18}F-choline PET/CT also detects malignant skeletal involvement. Currently, new PET tracers are being evaluated both in preclinical and clinical studies, and several of these imaging agents are demonstrating promising results.

MRI of the prostate provides a multiparametric view of anatomy and physiology. T1- and T2-weighted MRI provide unsurpassed anatomic resolution, especially at higher field strength and with the use of endorectal coils. DW-MRI provides insight into water diffusion with the prostate, which in turn, reflects cellularity and aggressiveness. MRS provides metabolic maps of prostate tissue, providing insight into biochemical disruption in cancers. DCE-MRI provides a map of tumor blood flow and permeability to low-molecular-weight contrast agents; tumors are associated with neoangiogenic vessels that enhance and washout early compared with normal tissue. Additionally, MRI can provide an overview of the retroperitoneum for lymphadenopathy, bone metastases, and coexistent tumors that could influence patient management. In short, MRI is a highly flexible modality. Despite these advantages, MRI often misses small tumors, and its ability to characterize tumor aggressiveness is not always accurate. For this reason, the results of MRI need to be complemented with other modalities such as PET scans, and most specifically, with image-guided tissue biopsy.

References

Papers of particular interest, published recently, have been highlighted as:

• Of importance

•• Of major importance

1••. Damber JE, Aus G. Prostate cancer. Lancet. 2008; 371:1710–1721. This article offers an excellent review on prostate cancer. [PubMed: 18486743]

2. Lassi K, Dawson NA. Emerging therapies in castrate-resistant prostate cancer. Curr Opin Oncol. 2009; 21:260–265. [PubMed: 19363343]

3•. Bouchelouche K, Capala J, Oehr P. Positron emission tomography/computed tomography and radioimmunotherapy of prostate cancer. Curr Opin Oncol. 2009; 21:469–474. This review briefly summarizes recent advances in PET/CT imaging and radioimmunotherapy of prostate cancer. [PubMed: 19535981]

4•. Bouchelouche K, Capala J. 'Image and treat': an individualized approach to urological tumors. Curr Opin Oncol. 2010 This short review discusses targets for personalized medicine with radionuclides. 10.1097/CCO.0b013e3283373d5c

5••. Kelloff GJ, Choyke P, Coffey DS. Challenges in clinical prostate cancer: role of imaging. AJR Am J Roentgenol. 2009; 192:1455–1470. Results from a recent workshop on prostate cancer and imaging technology are reviewed. The workshop was arranged by the Cancer Imaging Program of the National Cancer Institute, National Institutes of Health, Bethesda, USA. [PubMed: 19457806]

6•. Turkbey B, Albert PS, Kurdziel K, Choyke PL. Imaging localized prostate cancer: current approaches and new developments. AJR Am J Roentgenol. 2009; 192:1471–1480. This article discusses recent developments in imaging technologies, particularly MRI and PET/CT, which may lead to improved lesion detection and staging of prostate cancer. [PubMed: 19457807]

7•. Apolo AB, Pandit-Taskar N, Morris MJ. Novel tracers and their development for the imaging of metastatic prostate cancer. J Nucl Med. 2008; 49:2031–2041. In this article, recent advances in radiotracers for molecular imaging of advanced prostate cancer are described. [PubMed: 18997047]

8•. Turkbey B, Pinto PA, Choyke PL. Imaging techniques for prostate cancer: implications for focal therapy. Nat Rev Urol. 2009; 6:191–203. The authors review the advantages and disadvantages of conventional imaging techniques, developments for targeted imaging, and the possible role of image-guided biopsy and therapy for localized prostate cancer. [PubMed: 19352394]

9. Bouchelouche K, Oehr P. Positron emission tomography and positron emission tomography/computerized tomography of urological malignancies: an update review. J Urol. 2008; 179:34–45. [PubMed: 17997425]

10. Jana S, Blaufox MD. Nuclear medicine studies of the prostate, testes, and bladder. Semin Nucl Med. 2006; 36:51–72. [PubMed: 16356796]

11. Toth G, Lengyel Z, Balkay L, et al. Detection of prostate cancer with 11C-methionine positron emission tomography. J Urol. 2005; 173:66–69. [PubMed: 15592030]

12. Schuster DM, Votaw JR, Nieh PT, et al. Initial experience with the radiotracer anti-1-amino-3-18F-fluorocyclobutane-1-carboxylic acid with PET/CT in prostate carcinoma. J Nucl Med. 2007; 48:56–63. [PubMed: 17204699]

13. Dehdashti F, Picus J, Michalski JM, et al. Positron tomographic assessment of androgen receptors in prostatic carcinoma. Eur J Nucl Med Mol Imaging. 2005; 32:344–350. [PubMed: 15726353]

14••. Elsasser-Beile U, Buhler P, Wolf P. Targeted therapies for prostate cancer against the prostate specific membrane antigen. Curr Drug Targets. 2009; 10:118–125. This is an excellent review on the development of PSMA-targeted therapies. [PubMed: 19199907]

15••. Bouchelouche K, Choyke PL, Capala J. Prostate specific membrane antigen—a target for imaging and therapy with radionuclides. Discov Med. 2010; 9:55–61. PSMA is a promising target for an "image and treat" strategy with radionuclides. [PubMed: 20102687]

16. Milowsky MI, Nanus DM, Kostakoglu L, et al. Phase I trial of yttrium-90-labeled anti-prostate-specific membrane antigen monoclonal antibody J591 for androgen-independent prostate cancer. J Clin Oncol. 2004; 22:2522–2531. [PubMed: 15173215]

17. Bander NH, Milowsky MI, Nanus DM, et al. Phase I trial of 177lutetium-labeled J591, a monoclonal antibody to prostate-specific membrane antigen, in patients with androgen-independent prostate cancer. J Clin Oncol. 2005; 23:4591–4601. [PubMed: 15837970]

18. Wolf P, Freudenberg N, Buhler P, et al. Three conformational antibodies specific for different PSMA epitopes are promising diagnostic and therapeutic tools for prostate cancer. Prostate. 2010; 70:562–569. [PubMed: 19938014]

19•. Regino CA, Wong KJ, Milenic DE, et al. Preclinical evaluation of a monoclonal antibody (3C6) specific for prostate-specific membrane antigen. Curr Radiopharm. 2009; 2:9–17. The authors present a new mAb for PSMA imaging. [PubMed: 20047017]

20••. Elsasser-Beile U, Reischl G, Wiehr S, et al. PET imaging of prostate cancer xenografts with a highly specific antibody against the prostate-specific membrane antigen. J Nucl Med. 2009; 50:606–611. The antibody, mAb 3/A12, labeled with 64Cu, was used in this in vivo study for PET imaging of PSMA-positive tumors. [PubMed: 19289418]

21••. Hillier SM, Maresca KP, Femia FJ, et al. Preclinical evaluation of novel glutamate-urea-lysine analogues that target prostate-specific membrane antigen as molecular imaging pharmaceuticals for prostate cancer. Cancer Res. 2009; 69:6932–6940. This article discusses two promising agents, MIP-1072 and MIP 1095, for imaging PSMA-positive cancer. [PubMed: 19706750]

22••. Kramer-Marek G, Kiesewetter DO, Capala J. Changes in HER2 expression in breast cancer xenografts after therapy can be quantified using PET and 18F-labeled affibody molecules. J Nucl Med. 2009; 50:1131–1139. Affibody molecules labeled with 18F can be used to assess HER2 expression in vivo by PET, and monitor possible changes of receptor expression in response to therapeutic interventions. [PubMed: 19525458]

23. Farsad M, Schiavina R, Castellucci P, et al. Detection and localization of prostate cancer: correlation of (11)C-choline PET/CT with histopathologic step-section analysis. J Nucl Med. 2005; 46:1641–1649.

24. Scher B, Seitz M, Albinger W, et al. Value of 11C-choline PET and PET/CT in patients with suspected prostate cancer. Eur J Nucl Med Mol Imaging. 2007; 34:45–53. [PubMed: 16932935]

25. Cimitan M, Bortolus R, Morassut S, et al. [(18)F]fluorocholine PET/CT imaging for the detection of recurrent prostate cancer at PSA relapse: experience in 100 consecutive patients. Eur J Nucl Med Mol Imaging. 2006; 33:1387–1398. [PubMed: 16865395]

26••. Castellucci P, Fuccio C, Nanni C, et al. Influence of trigger PSA and PSA kinetics on 11C-Choline PET/CT detection rate in patients with biochemical relapse after radical prostatectomy. J Nucl Med. 2009; 50:1394–1400. The authors showed that the PET/CT detection rate of prostate cancer recurrence is influenced by trigger PSA and PSA kinetics. This may have clinical implications. [PubMed: 19690023]

27. Albrecht S, Buchegger F, Soloviev D, et al. (11)C-acetate PET in the early evaluation of prostate cancer recurrence. Eur J Nucl Med Mol Imaging. 2007; 34:185–196. [PubMed: 16832632]

28. Even-Sapir E, Metser U, Mishani E, et al. The detection of bone metastases in patients with high-risk prostate cancer: 99mTc-MDP Planar bone scintigraphy, single- and multi-field-of-view SPECT, 18F-fluoride PET, and 18F-fluoride PET/CT. J Nucl Med. 2006; 47:287–297. [PubMed: 16455635]

29••. Beheshti M, Vali R, Waldenberger P, et al. Detection of bone metastases in patients with prostate cancer by (18)F fluorocholine and (18)F fluoride PET-CT: a comparative study. Eur J Nucl Med Mol Imaging. 2008; 35:1766–1774. This prospective study compared 18F-fluorocholine and 18F-fluoride PET/CT for the detection of bone metastases from prostate cancer. [PubMed: 18465129]

30. Swindle P, Eastham JA, Ohori M, et al. Do margins matter? The prognostic significance of positive surgical margins in radical prostatectomy specimens. J Urol. 2008; 179:S47–S51. [PubMed: 18405751]

31. el-Gabry EA, Halpern EJ, Strup SE, Gomella LG. Imaging prostate cancer: current and future applications. Oncology (Williston Park). 2001; 15:325–336. [PubMed: 11301831]

32. Hocht S, Wiegel T, Bottke D, et al. Computed tomogram prior to prostatectomy. Advantage in defining planning target volumes for postoperative adjuvant radiotherapy in patients with stage C prostate cancer? Strahlenther Onkol. 2002; 178:134–138. [PubMed: 11962189]

33. Akin O, Sala E, Moskowitz CS, et al. Transition zone prostate cancers: features, detection, localization, and staging at endorectal MR imaging. Radiology. 2006; 239:784–792. [PubMed: 16569788]

34. Scheidler J, Hricak H, Vigneron DB, et al. Prostate cancer: localization with three-dimensional proton MR spectroscopic imaging—clinicopathologic study. Radiology. 1999; 213:473–480. [PubMed: 10551229]

35. Wefer AE, Hricak H, Vigneron DB, et al. Sextant localization of prostate cancer: comparison of sextant biopsy, magnetic resonance imaging and magnetic resonance spectroscopic imaging with step section histology. J Urol. 2000; 164:400–404. [PubMed: 10893595]

36. Ikonen S, Kivisaari L, Tervahartiala P, et al. Prostatic MR imaging. Accuracy in differentiating cancer from other prostatic disorders. Acta Radiol. 2001; 42:348–354. [PubMed: 11442457]

37. Kwek JW, Thng CH, Tan PH, et al. Phased-array magnetic resonance imaging of the prostate with correlation to radical prostatectomy specimens: local experience. Asian J Surg. 2004; 27:219–224. [PubMed: 15564165]

38. Nakashima J, Tanimoto A, Imai Y, et al. Endorectal MRI for prediction of tumor site, tumor size, and local extension of prostate cancer. Urology. 2004; 64:101–105. [PubMed: 15245944]

39. Yamaguchi T, Lee J, Uemura H, et al. Prostate cancer: a comparative study of 11C-choline PET and MR imaging combined with proton MR spectroscopy. Eur J Nucl Med Mol Imaging. 2005; 32:742–748. [PubMed: 16052370]

40. Cirillo S, Petracchini M, Scotti L, et al. Endorectal magnetic resonance imaging at 1. 5 Tesla to assess local recurrence following radical prostatectomy using T2-weighted and contrast-enhanced imaging. Eur Radiol. 2009; 19:761–769. [PubMed: 18825386]

41. Sala E, Eberhardt SC, Akin O, et al. Endorectal MR imaging before salvage prostatectomy: tumor localization and staging. Radiology. 2006; 238:176–183. [PubMed: 16373766]

42. Tan JS, Thng CH, Tan PH, et al. Local experience of endorectal magnetic resonance imaging of prostate with correlation to radical prostatectomy specimens. Ann Acad Med Singapore. 2008; 37:40–43. [PubMed: 18265896]

43. Futterer JJ, Engelbrecht MR, Huisman HJ, et al. Staging prostate cancer with dynamic contrast-enhanced endorectal MR imaging prior to radical prostatectomy: experienced versus less experienced readers. Radiology. 2005; 237:541–549. [PubMed: 16244263]

44. Bloch BN, Furman-Haran E, Helbich TH, et al. Prostate cancer: accurate determination of extracapsular extension with high-spatial-resolution dynamic contrast-enhanced and T2-weighted MR imaging—initial results. Radiology. 2007; 245:176–185. [PubMed: 17717328]

45••. Weinreb JC, Blume JD, Coakley FV, et al. Prostate cancer: sextant localization at MR imaging and MR spectroscopic imaging before prostatectomy—results of ACRIN prospective multi-

institutional clinicopathologic study. Radiology. 2009; 251:122–133. This prospective multicenter study compared the benefit of T2W MR imaging and MR spectroscopy versus T2W MR imaging alone. [PubMed: 19332850]

46. Issa B. In vivo measurement of the apparent diffusion coefficient in normal and malignant prostatic tissues using echo-planar imaging. J Magn Reson Imaging. 2002; 16:196–200. [PubMed: 12203768]
47. Tamada T, Sone T, Jo Y, et al. Prostate cancer: relationships between postbiopsy hemorrhage and tumor detectability at MR diagnosis. Radiology. 2008; 248:531–539. [PubMed: 18539890]
48. Kim CK, Park BK, Lee HM, Kwon GY. Value of diffusion-weighted imaging for the prediction of prostate cancer location at 3 T using a phased-array coil: preliminary results. Invest Radiol. 2007; 42:842–847. [PubMed: 18007156]
49. Miao H, Fukatsu H, Ishigaki T. Prostate cancer detection with 3-T MRI: comparison of diffusion-weighted and T2-weighted imaging. Eur J Radiol. 2007; 61:297–302. [PubMed: 17085002]
50. Haider MA, van der Kwast TH, Tanguay J, et al. Combined T2-weighted and diffusion-weighted MRI for localization of prostate cancer. AJR Am J Roentgenol. 2007; 189:323–328. [PubMed: 17646457]
51. Kozlowski P, Chang SD, Jones EC, et al. Combined diffusion-weighted and dynamic contrast-enhanced MRI for prostate cancer diagnosis—correlation with biopsy and histopathology. J Magn Reson Imaging. 2006; 24:108–113. [PubMed: 16767709]
52. Reinsberg SA, Payne GS, Riches SF, et al. Combined use of diffusion-weighted MRI and 1H MR spectroscopy to increase accuracy in prostate cancer detection. AJR Am J Roentgenol. 2007; 188:91–98. [PubMed: 17179350]
53. Mazaheri Y, Shukla-Dave A, Hricak H, et al. Prostate cancer: identification with combined diffusion-weighted MR imaging and 3D 1H MR spectroscopic imaging—correlation with pathologic findings. Radiology. 2008; 246:480–488. [PubMed: 18227542]
54. Kurhanewicz J, Vigneron DB, Hricak H, et al. Three-dimensional H-1 MR spectroscopic imaging of the in situ human prostate with high (0.24–0. 7-cm3) spatial resolution. Radiology. 1996; 198:795–805. [PubMed: 8628874]
55. Zakian KL, Sircar K, Hricak H, et al. Correlation of proton MR spectroscopic imaging with Gleason score based on step-section pathologic analysis after radical prostatectomy. Radiology. 2005; 234:804–814. [PubMed: 15734935]
56. Tofts PS, Brix G, Buckley DL, et al. Estimating kinetic parameters from dynamic contrast-enhanced T(1)-weighted MRI of a diffusable tracer: standardized quantities and symbols. J Magn Reson Imaging. 1999; 10:223–232. [PubMed: 10508281]
57. Concato J, Jain D, Li WW, et al. Molecular markers and mortality in prostate cancer. BJU Int. 2007; 100:1259–1263. [PubMed: 17850375]
58. Noworolski SM, Vigneron DB, Chen AP, Kurhanewicz J. Dynamic contrast-enhanced MRI and MR diffusion imaging to distinguish between glandular and stromal prostatic tissues. Magn Reson Imaging. 2008; 26:1071–1080. [PubMed: 18508221]
59••. Ocak I, Bernardo M, Metzger G, et al. Dynamic contrast-enhanced MRI of prostate cancer at 3 T: a study of pharmacokinetic parameters. AJR Am J Roentgenol. 2007; 189:849. This prospective study showed that specificity of prostate MRI at 3T for prostate cancer is improved by performing DCE-MRI and using pharmacokinetic parameters. [PubMed: 17885055]
60. Kim JK, Hong SS, Choi YJ, et al. Wash-in rate on the basis of dynamic contrast-enhanced MRI: usefulness for prostate cancer detection and localization. J Magn Reson Imaging. 2005; 22:639–646. [PubMed: 16200542]
61. Villers A, Puech P, Mouton D, et al. Dynamic contrast enhanced, pelvic phased array magnetic resonance imaging of localized prostate cancer for predicting tumor volume: correlation with radical prostatectomy findings. J Urol. 2006; 176:2432–2437. [PubMed: 17085122]
62. Cheikh AB, Girouin N, Colombel M, et al. Evaluation of T2-weighted and dynamic contrast-enhanced MRI in localizing prostate cancer before repeat biopsy. Eur Radiol. 2009; 19:770–778. [PubMed: 18925403]

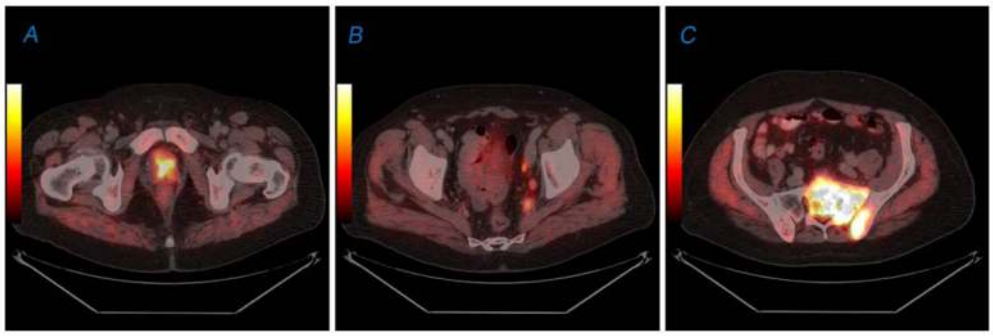

Fig. 1.
Preoperative ^{18}F-choline PET/CT staging of a 63-year-old man with prostate cancer. Axial-fused PET/CT images demonstrate pathological ^{18}F-choline uptake in the prostate (**a**), in three pelvic lymph nodes (**b**), and in bones (**c**). *CT* computed tomography; *PET* positron emission tomography

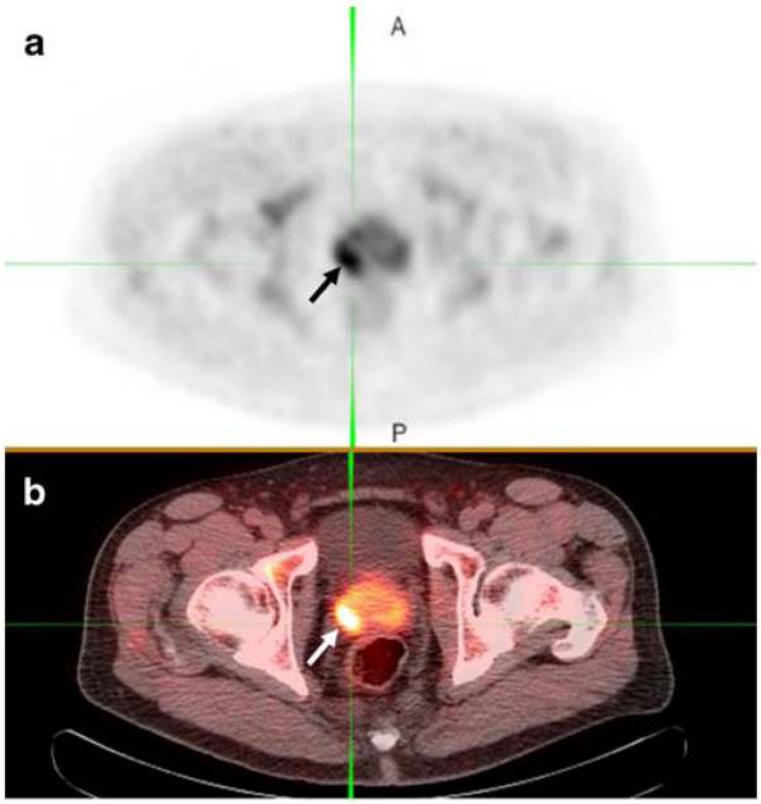

Fig. 2.
^{11}C-acetate PET (**a**) and PET/CT (**b**) images of a 58-year-old man with prostate cancer demonstrate pathological uptake in the right mid peripheral zone (*arrows*) consistent with a Gleason 7 prostate cancer lesion. *CT* computed tomography; *PET* positron emission tomography

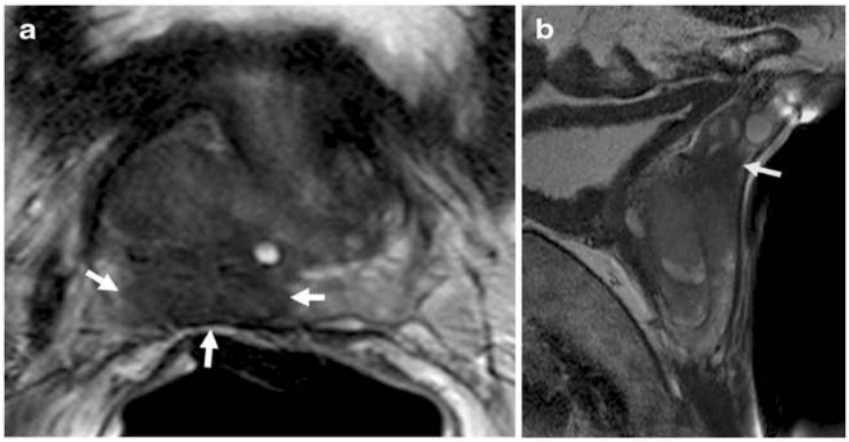

Fig. 3.

Axial and sagittal T2-weighted MR images of a 58-year-old man with prostate cancer demonstrate a big peripheral zone tumor (*white arrows*), which obliterates the right rectoprostatic angle suggesting extracapsular extension (**a**) and extends superiorly and invading seminal vesicles (*arrow*) (**b**). *T* Tesla

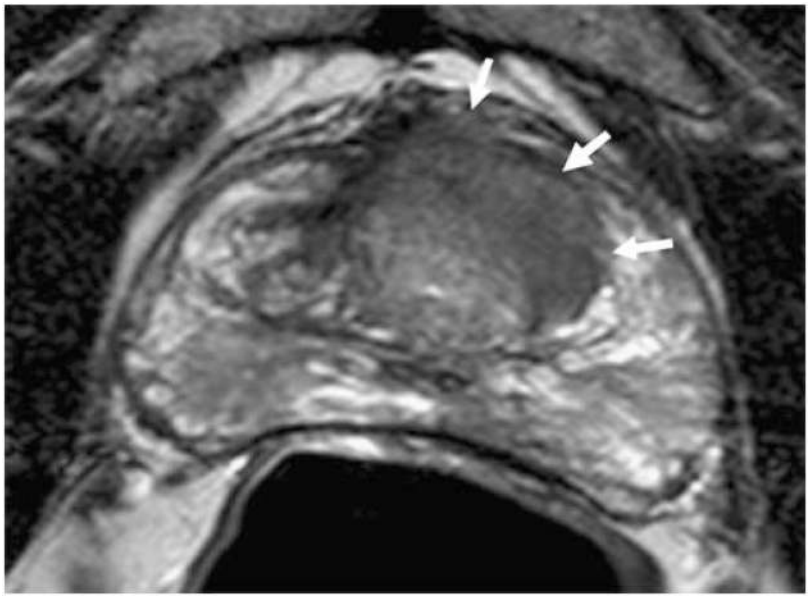

Fig. 4.

Axial T2-weighted MR image of a 65-year-old man with prostate cancer shows a lenticular shaped, low-intermediate signal intensity lesion with irregular speculated margins in the left mid transition zone consistent with a left anterior transition zone cancer of the prostate (*white arrows*). *T* Tesla

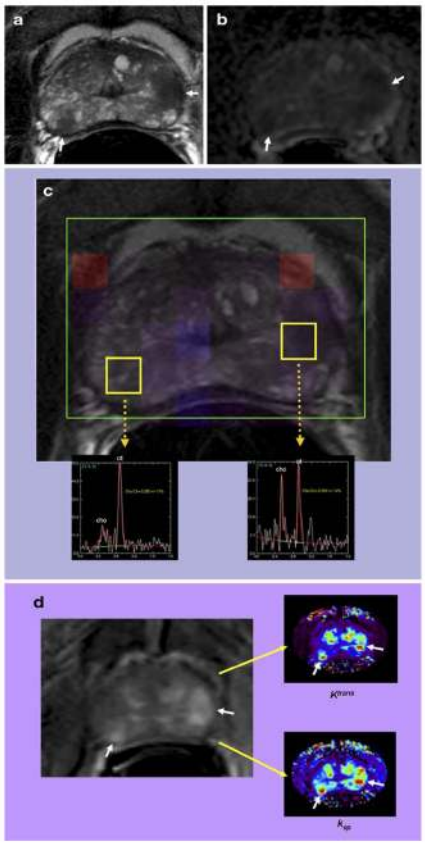

Fig. 5.

A 61-year-old man with prostate cancer. Axial T2W MR image demonstrates bilateral low signal intensity lesions at the peripheral zone (*arrows*) (**a**); lesions demonstrate diffusion restriction on corresponding apparent diffusion coefficient map of DW-MRI (*arrows*) (**b**); MR spectroscopy demonstrates increased choline-to-citrate ratio within bilateral peripheral zone lesions (**c**); lesions show increased enhancement on axial T1W DCE-MR image, whereas color-coded K^{trans} and k_{ep} maps delineate both tumor lesions (*arrows*) (**d**). *DCE-MRI* dynamic contrast-enhanced MRI; *DW-MRI* diffusion-weighted MRI; *T* Tesla